METHODOLOGY AND PRELIMINARY RESULTS OF UNSATURATED-FLOW STUDIES FOR A PROPOSED LOW-LEVEL RADIOACTIVE WASTE DISPOSAL FACILITY, TEXAS

Bridget Scanlon, F. P. Wang, and B. C. Richter

Prepared for

Texas Low-Level Radioactive Waste Disposal Authority

under Interagency Contract Number IAC(88-89)-0932

Bureau of Economic Geology

W. L. Fisher, Director

The University of Texas at Austin

Austin, Texas 78713

August 1989

ABSTRACT

Site characterization studies are being conducted for low-level radioactive waste disposal in an area 35 mi (65 km) southeast of El Paso, Texas. An important factor in evaluation of site suitability for waste disposal is estimation of the direction and rate of moisture movement through the thick unsaturated zone. Physical and chemical approaches were used to evaluate moisture movement in the unsaturated zone. Physical methods include monitoring moisture content with a neutron probe and monitoring water potential with psychrometers. Chemical tracers such as bomb ^{36}Cl were used to evaluate recharge rates over a longer period (approximately 30 yr).

The lack of temporal variations in moisture content and the low water potentials indicate that water movement through the unsaturated zone is minimal and is primarily restricted to upward vapor movement, probably controlled by evapotranspiration. Recharge estimates from the chemical tracers are also minimal, less than 1% of the mean annual precipitation rate.

INTRODUCTION

This study is part of a larger program to evaluate site characteristics for a proposed low-level radioactive waste disposal facility in Texas (fig. 1). The unsaturated zone in the Chihuahuan desert is being considered as a site for a potential repository of low-level radioactive waste. Regulatory guidelines for disposal of such waste were established by the U. S. Nuclear Regulatory Commission and are outlined in 10 CFR 61 (Office of the Federal Register, 1987), NUREG 0902 (Siefken and others, 1982), and NUREG 1200 (U.S. Nuclear Regulatory Commission, 1987). According to these regulations, the waste must be isolated from the accessible environment for 500 yr. Unsaturated near-surface disposal sites (< 66 ft [20 m] below land surface) are preferred for disposal of the waste

(NUREG 0902). Water and vapor movement are recognized as the primary pathways for radionuclide transport. The purpose of our study is to determine the potential for radionuclide transport by evaluating the predominant direction and rate of water and/or vapor movement in the unsaturated zone. Physical and chemical approaches were used to evaluate water movement in the unsaturated zone. Physical methods included monitoring the moisture content and water potential and measuring the hydraulic conductivity and moisture-retention characteristics of the sediments. Chemical methods involved using ^{35}Cl, ^{36}Cl, and ^{3}H to evaluate recharge rates.

Potential pathways for waste migration include (1) water infiltration into the facility, leaching of radioactive material, and transport to the water table and/or (2) surface erosion and transport of radioactive material in runoff (fig. 2). Vapor transport to the surface is not considered a critical pathway because the majority of radioactive isotopes are nonvolatile, except for carbon, oxygen, and hydrogen. The disposal facility will be installed to a depth of approximately 40 ft (12 m) and will occupy an area of approximately 50 acres (202,500 m^2). Radioactive material will be in a solid form and will be disposed of in cannisters. An engineered barrier will be used to prohibit radionuclide migration from the facility. Although the facility will be designed to contain the waste, reliance will be placed on the natural system to contain the waste for the 500-yr time period. This report outlines our methodology and preliminary results.

Setting

The site is located in the Chihuahuan desert within the Basin and Range physiographic province approximately 35 mi (65 km) southeast of El Paso (fig. 1a). The Hueco Bolson is a large basin within the Chihuahuan desert that encompasses the site. The Diablo Plateau (approximately 1.6 mi [3 km] northeast of the site) consists of Cretaceous rocks and forms a steep escarpment (fig. 1b). The topography at the site is relatively flat

with slopes of less than 1 % (fig. 1). Two main drainages border the site, Alamo Arroyo to the northwest and Camp Rice Arroyo to the southeast. The arroyos drain southwestward to the Rio Grande and are generally dry except after rainfall events. The unsaturated zone consists of 40 ft to 50 ft (12 to 15 m) of lacustrine and alluvial sandy and gravelly loam of the Pleistocene Camp Rice Formation underlain by approximately 460 ft (140 m) of lacustrine clays with interbedded silts and sands of the Pleistocene Fort Hancock Formation (Gustavson, 1989). A discontinuous layer of caliche occurs at a depth of approximately 6 ft (2 m). Surficial sediments consist of wind-blown sandy loam in dunes and interfluves, loam in fluvial areas and sandy gravel in upland areas (R. W. Baumgardner, Jr., personal communication, 1989) (fig. 3). Extreme local variations in sediment texture were observed in trenches dug to a depth of 12 m. Shrubs such as creosote (*Larrea tridentata*) and mesquite (*Prosopis glandulosa*) are common with rooting depths of 3 ft to 16 ft (1 to 5 m).

Regional climate, monitored at Fort Hancock and El Paso, is subtropical arid (Larkin and Bomar, 1983), with average annual precipitation of approximately 11 inches (280 mm). Approximately 60 % of the precipitation falls as local, intense, short-duration convective storms between June and September, when temperature and potential evaporation are highest (fig. 4). Minor winter frontal storms are of longer duration. Mean annual temperature is approximately 17 °C, whereas monthly mean temperatures range from 5°C in December to 28°C in July. Mean annual class-A pan evaporation is approximately seven times mean annual precipitation. High-intensity precipitation results in surface runoff with very spiky patterns (fig. 5). These climatic and hydrograph data suggest that water movement through the unsaturated zone is minimal because most water either runs off or evaporates. Mean annual snowfall of approximately 0.4 inch (10 mm) may provide a mechanism for recharge because evaporation is low during the winter.

Potential Measurements

Although temporal variations in moisture content are used to evaluate the movement of recharge pulses through the unsaturated zone, moisture content is discontinuous across different materials, and variations in moisture content with depth do not provide information on the direction of water movement. In contrast, energy potential is continuous across different materials, and the potential gradient is used to assess the direction and rate of water flow under isothermal conditions. Water flows from regions of high to low total potential. Total potential (ψ_T) in the unsaturated zone consists of the following components:

$$\psi_T = \psi_m + \psi_g + \psi_\pi - \psi_p \qquad (1)$$

where ψ_m, ψ_g, ψ_π, and ψ_p are the matric, gravitational, osmotic, and pressure potentials, respectively. High matric potentials (> - 0.1 MPa) result primarily from capillary forces whereas low matric potentials (< -0.1 MPa) result from water adsorbed on grain surfaces. Gravitational potential is the elevation above the water table, which is used as a reference datum. Osmotic potential is associated with solutes in the water and the pressure potential results from external pressure on water in the system. Osmotic and pressure potentials are generally negligible and can be ignored.

Various instruments are used to measure potential energy, depending on its range. Tensiometers are restricted to matric potential measurements in the effective range of 0 to -0.08 MPa. Psychrometers measure the relative humidity (p/p_o), which is proportional to water (matric and osmotic) potential (ψ) according to the Kelvin equation:

$$\psi = (RT/V_W) \ln(p/p_o) \qquad (2)$$

where ψ is in MPa, R is the ideal gas constant (8.3143 J K^{-1} mol^{-1}), and Vw is the molar volume of water ($1.8 \cdot 10^{-5} m^3$ mol^{-1}) (Rawlins and Campbell, 1986). The relative humidity is measured by the wet bulb temperature depression. The temperature of the wet bulb is measured relative to that of a dry bulb at the sample surface. Temperature

gradients, whether in a laboratory system or natural gradients near the soil surface, are extremely critical because a 1°C temperature difference at 20°C between the dry bulb and the sample results in a measurement error of 13 MPa (Rawlins and Campbell, 1986). *In situ* soil psychrometers (fig. 6) are Spanner-type psychrometers that use the Peltier effect to condense water in the psychrometer (Spanner, 1951). The laboratory psychrometer used in the present study (fig. 7) is a Richards-type psychrometer in which a drop of water is mechanically added to the thermocouple. The temperature depression of the wet bulb is translated into output voltage using the Seebeck effect. The Richards-type psychrometer can span a much larger range (-0.2 to -300 MPa) (Rawlins and Campbell, 1986) in water potentials than the Spanner type (-0.2 to -8 MPa) because the Peltier effect cannot condense water below approximately -0.8 MPa. The copper constantan junction in the thermocouple is used to measure temperature.

PHYSICAL APPROACH

Field Methods

Neutron thermalization was used to monitor moisture content and tensiometers and psychrometers were used to monitor water potential (figs. 8 and 9). All the monitoring equipment was installed in an ephemeral stream because recharge rates should be greater in this setting than in interfluvial areas. In addition to data gathered by field monitoring, samples were collected from various geomorphic settings for laboratory measurements of moisture content, water potential, moisture retention, and grain-size distribution. Saturated and unsaturated hydraulic conductivity were determined both in the field and in the laboratory. A compilation of boreholes drilled, monitoring equipment installed, and samples collected is presented in table 1.

Moisture Content

Soil samples were collected for gravimetric moisture content. These samples were placed in polyethylene containers that were sealed with parafilm and tape to avoid moisture loss, and weighed in the field. Except for the deeper clays, the soils were generally not sufficiently cohesive to collect undisturbed samples for volumetric-moisture-content and bulk-density analyses. In the shallow zone, therefore, volumetric-moisture and bulk-density samples were collected in brass cylinders after ponding different sites for unsaturated and saturated hydraulic-conductivity tests.

To install neutron-probe access tubes, two boreholes (70 and 135 ft [21 and 41 m] deep) were drilled approximately 20 ft (6 m) apart with an air rotary rig (figs. 8 and 9). The boreholes were drilled with a drag bit using a 60 kg hammer (Mullican and others, 1989). Because of difficulty drilling through the sediments, steel drill pipe was used instead of conventional aluminum access tubes. The access tubing was driven with a 180 kg hammer and advanced every 10 ft (3 m) to avoid drying the overlying material during drilling. The top 70 ft (21 m) of the deeper borehole was cemented for stability. Cement was poured at the surface around the access tubes to avoid erosion during surface-water runoff and to prevent downward flow around the access tubes. Several other shallow boreholes (61 - 63) were drilled to depths of 6 ft (1.8 m) with a solid-stem auger for installation of neutron-probe access tubes. Borehole 61 was drilled in an ephemeral pond that drains slowly after rainfall events.

Moisture content is monitored approximately monthly using a CPN model 503 DR neutron probe. Readings are made at approximately 1 ft (0.3 m) intervals to a depth of 10 ft (3 m) and at 3 ft (1 m) intervals to a depth of 135 ft (41 m). Moisture content also is monitored monthly in the shallow access tubes at 0.3 ft (0.1 m) intervals from 1 ft (0.3 m) to 3 ft (1 m) depths. Whenever possible, moisture content is measured daily at shallow levels after rainfall events. The shallowest monitoring depth is controlled by the radius of

influence (r, in m) of the neutron probe, which is dependent upon the moisture content and can be calculated according to the following formula (van Bavel and others, 1956):

$$r = 0.15\ \theta^{-0.33}$$

This depth ranges from approximately 0.9 to 1.1 ft (0.28 to 0.33 m) in the study area.

Calibration of the neutron probe involved installation of two neutron access tubes (6 ft [1.8 m] deep), one in a plot that was ponded for an instantaneous profile test and the other offset by approximately 30 ft (10 m) in a dry area. Neutron counts were recorded at approximately 0.3-ft (0.1-m) intervals from a depth of 1 to 6 ft (0.3 to 1.2 m). A 15 s counting time was used. Soil samples were collected in brass cylinders using a double cylinder, hammer-driven core sampler (Soil Moisture Equipment, Inc.) at the same depth intervals adjacent to the access tube. The samples were weighed in the field. Volumetric moisture content was determined in the laboratory using standard methods. The calibration curve was calculated by least-squares linear regression of the volumetric moisture content and neutron counts.

$$q = -6.4674 + 0.003912\ Cn \qquad (4)$$

where θ is the volumetric moisture content and Cn is the neutron count/min (fig. 10).

Potential Energy

Tensiometers, used to measure matric potential, were obtained from Soil Measurement Systems and consisted of plastic tubing with a porous ceramic cup at one end and a septum stopper at the other. Tensiometers were installed using a hollow stem pipe (1 inch [25 mm] diameter) that was pushed into the ground with the Mobile drill rig. A slurry was made with sieved material from the boreholes to provide a good contact between the tensiometer cup and the surrounding sediments. A tensimeter, which is a hand-held pressure transducer with a digital readout (sensitivity $1 \cdot 10^{-4}$ MPa), was used to measure tension in the tensiometers (Marthaler and others, 1983). The tensimeter was calibrated by

the manufacturers against a hanging water column. Tensiometers installed at 3, 5, and 6 ft (0.9, 1.5, and 1.8 m) (figs. 8 and 9) to monitor natural potentials were not operational because the matric potential was too low (< -0.08 MPa). However, areas ponded for the instantaneous profile test had matric potentials within the range measured by tensiometers.

Psychrometers were installed in the field in March 1989 (figs. 8 and 9). To install psychrometers at shallow depths, a pit was dug to 4.6 ft (1.4 m) with a shovel, and the psychrometers were emplaced in holes drilled laterally into the pit wall to ensure that material overlying the psychrometers is undisturbed and to provide a good contact between the psychrometers and the surrounding sediments. These holes were sealed with native material. The psychrometers were placed so that their symmetry axis is perpendicular to temperature gradients to minimize the effect of such gradients on psychrometer output. Psychrometers were installed in duplicate for data verification at depths of 1 ft (0.3 m) and at 1-ft (0.3-m) intervals between depths of 1.6 and 4.6 ft (0.5 and 1.4 m). Campbell CS107 (Campbell Scientific, Inc.) thermistors were installed at 0.3-ft (0.1-m) intervals from depths of 0.6 and 2 ft (0.2 and 0.6 m) to record soil temperature. The pit was backfilled with the original sediments.

To install psychrometers at greater depths, a borehole was drilled to a depth of 48 ft (14.5 m) with a solid stem auger (2 inch [50 mm] diameter) (figs. 8 and 9). Wetting or drying of native material is expected to be minimal because no drilling fluid was used. The psychrometers were emplaced in a PVC screen filled with commercial (Ottawa) sand to protect them during installation. Because the psychrometers were not retrievable, they were installed in duplicate at each of the following depths: 9 ft (2.7 m), 15 ft (4.6 m), 25 ft (7.6 m), 34 ft (10.5 m), and 47 ft (14.3 m) (fig. 11). Material removed during drilling was labeled according to depth and stored in PVC buckets. Cuttings from the borehole were used to backfill immediately around the psychrometers; however, the material from depths shallower than 20 ft (6 m) was considered too coarse, and commercial Ottawa sand was used at these levels. Epoxy was used to prevent preferential gas flow between

psychrometer stations and as a seal at the surface to minimize preferential flow down the borehole. Epoxy was chosen because it does not introduce water into the system. Properties of the epoxy that are important in psychrometer installation are the curing time (1 to 2 hr), viscosity (2 to 20 poises), and a curing temperature (< 50 °C). Epoxy DER324/DEH24 from Dow Chemical Company was tested and used. The cuttings were poured down one tremie pipe and the epoxy down another. The small-diameter borehole and the backfill with natural materials were designed to minimize psychrometer equilibration time.

Temperature measurements are recorded with the chromel constantan junction of the thermocouple psychrometer and with thermistors. The psychrometers and thermistors are connected to a Campbell CR7 data logger (Campbell Scientific, Inc.). The data logger is powered with a solar panel and a rechargeable internal battery. An external marine battery is used for backup. Water potentials and temperatures are logged daily at 0900 hr. Hourly data are recorded for 1 to 4 days each month. Data are downloaded monthly.

In addition to the use of tensiometers and psychrometers for monitoring water potential, soil samples were collected for water potential measurements in the laboratory (figs. 7 to 9). These samples were collected while boreholes were being drilled for installation of monitoring equipment such as soil solution samplers. The boreholes were drilled with a hollow stem auger (0.6 ft [0.2 m] diameter), and samples were collected in shelby tubes (3 inch [76 mm] diameter). Initially the shelby tubes were waxed with paraffin at both ends at the field site, and the samples were removed in the laboratory with an extruder; this was difficult where the shelby tubes were crinkled by drilling through gravel or caliche. Later, all samples were removed from the shelby tubes in the field with a pick and placed in mason jars. The lid of the jar was sealed with paraffin in the field to avoid moisture loss.

Hydraulic Conductivity

Saturated hydraulic conductivity was measured in the field using a Guelph permeameter (Soil Moisture Equipment, Inc.) (figs. 8 and 9). The instantaneous profile method was used to measure unsaturated hydraulic conductivity in the field (Watson, 1966) (figs. 8 and 9). A level 6 ft^2 (2 m^2) area free of vegetation was chosen for the test. A trench was dug around the test plot, and wood planks and plastic were used to isolate the test plot from the surrounding sediments. A neutron-probe access tube was installed in the center of the plot to monitor moisture content to a depth of 5 ft (1.6 m). Five sets of four tensiometers were installed at 1-ft (0.3-m) intervals to a depth of 5 ft (1.5 m) to measure matric potential. A hand drill was used in the top 2 ft (0.6 m), and a hollow steel pipe was used to install the deeper tensiometers. Boreholes were larger than the diameter of the tensiometer and were backfilled with native material; bentonite was placed at the surface to prevent downward leaking of water around the tensiometer. The plot was flooded for 15 hr. After cessation of ponding, the plot was covered with plastic and soil to minimize evaporation. Infiltration was estimated from the rate of decline of the ponded water. Moisture content and matric potential were measured during ponding and drainage.

Laboratory Methods

Water potential was measured in the laboratory with the Decagon psychrometer SC-10 sample changer (Decagon Inc.) (fig. 7). The psychrometer was calibrated with NaCl solutions of known osmotic potential (ψ_π). The osmotic potentials (ψ_π (MPa)) of the NaCl solutions were calculated according to the following formula (Campbell, 1985)

$$\psi_\pi = -1000(\upsilon C \chi R T) \qquad (5)$$

where υ is the number of osmotically active particles (2 for NaCl), C is the concentration (moles/kg), χ is the osmotic coefficient (Robinson and Stokes (1959), R is the gas constant

(8.3142 J $mole^{-1}$ K^{-1}), and T is the temperature (K). Osmotic potentials for certain molalities and certain temperatures are listed in Lang (1967). NaCl solutions were prepared according to procedures outlined in Brown and van Haveren (1972). The solutions ranged in concentration from 0.05 M to saturated and correspond to osmotic potentials of -0.2 to -38 MPa at 20°C. Initially 2 sets of 20 calibration solutions were prepared and measured and a regression line was drawn to test the instrument (fig. 12). Temperature is also recorded with the water potential so that microvolt output can be corrected to a constant temperature. Water potentials from -0.01 to -10 MPa correspond to relative humidities from 93 to 100 %; therefore, all measurements were conducted in a glove box lined with wet paper towels to minimize moisture loss from the samples. Temperature variations in the laboratory were minimal. During routine analyses, six samples were placed in the sample changer (fig. 7), and after 30 minutes (min) of temperature and vapor pressure equilibration the output was scanned to determine what bracketing standards should be run with the samples. The standards were then placed in the chamber, and after another 30 min the standards, the six samples, and finally the three standards were read. One-second (s) readings were recorded for a period of 120 s with a Terra8 data logger (Terra Systems, Inc.). Least-squares linear regression was used to calculate the sample water potential using the 120 s microvolt output. Three sets of samples (six samples each) were analyzed from the same mason jar and gave low standard deviations (mean water potential (wp) -8.9 MPa, σ 0.2 MPa; wp -4.2 MPa, σ 0.2 MPa; wp -2.8 MPa, σ 0.5 MPa). In addition, different equilibration times were also tested by analyzing a set of six samples at 1, 1.5, and 2.5 hr. These data showed that mean psychrometer output (8.9 MPa) was not affected by varying the equilibration time between 1 and 2.5 hr.

Erratic readings or nonconcurrence of the two sets of standard count readings indicate that the SC-10 is not functioning properly. The first step taken was to clean the thermocouple psychrometer and thermocouple mount with distilled de-ionized water and to dry them with canned compressed air. If this was not sufficient, the thermocouple was

replaced. Some problems with rotating the sample changer were rectified with Teflon dry lube.

Field psychrometers consisted of screen-caged, single-junction thermocouple psychrometers (fig. 5) (Model PST 55, Wescor Inc.) that were calibrated in the laboratory at five different water potentials and at three different temperatures prior to installation (table 1). Calibration procedures similar to those outlined in Brown and Bartos (1982) were followed. A Tronac refrigerated water bath (Model # PTC 41, Tronac Inc.) (1 σ temperature control of $1 \cdot 10^{-4}$ °C) was used to provide a constant temperature environment. Temperature of the water bath was recorded with thermistors, thermocouple psychrometers, and a mercury thermometer. Sodium-chloride solutions (0.2 to 1.5 molalities) were used as a source of known water potential. Psychrometer readings are dependent on the magnitude and duration of the cooling current. A Peltier cooling current of 5 milliamps (ma) is generally considered optimal (Brown and Bartos, 1972). Higher cooling currents cause adverse effects associated with joule heating of thermocouple wires. A 30 s cooling time is considered appropriate for general applications (Brown and Bartos, 1972). Shorter cooling times result in less precise water potential measurements, whereas longer cooling times do not extend the range of psychrometers more than 0.5 MPa and are therefore not considered advantageous. Condensation time, cooling current, and voltage endpoint determination were kept constant during calibration and field measurement of water potential; therefore, their effects should cancel.

To minimize heat conduction along the wires, approximately 1 m of lead wire was submerged in the water bath during calibration. Psychrometers were calibrated with the required cable lengths for field installation. Because the psychrometer lead wires were of different lengths, different cooling voltages were applied to obtain a 5 ma cooling current at the psychrometer tip. The required cooling currents were calculated according to the CR7 manual and measured with a milliampmeter. Psychrometers (up to four) with similar lead wire lengths were attached to each interface in the CR7 data logger because only one

cooling current could be applied to the psychrometers on an interface. In most cases four psychrometers were attached to each A3497 interface, resulting in a minimum time interval between readings of 1.2 s. Psychrometer output was recorded every hour during calibration with the data logger. Because psychrometer output may correspond to two different water potentials, at least 60 readings were recorded for each psychrometer to distinguish readings in the dry and wet range. Temperature equilibration is indicated by the null offset and is usually attained within 1 hr. Vapor pressure equilibration is attained when similar consecutive hourly readings are recorded.

Initially the psychrometers were suspended in test tubes filled with NaCl solution. Various materials including beeswax and parafilm were used to seal the thermocouple wires to the lid of the test tubes. Some of the psychrometers showed a slow decline in microvolt ouput during calibration, whereas others recorded a marked drop to zero within an hour. These reductions in output were attributed to leakage into test tubes and through psychrometer screens although screen cages were designed to prevent water movement to the psychrometer. Final calibrations were conducted in a sample chamber made of Swagelock copper fittings similar to those described in Brown and Bartos (1982) and using Whatman #1 filter paper saturated with NaCl solutions. Psychrometers were cleaned with warm soapy water between different molality solutions. The mean calibration curve calculated for 24 psychrometers at 15, 20, and 25°C is shown in figure 13.

Moisture Content, Bulk Density, and Porosity

Gravimetric and volumetric moisture content was determined by weighing and oven drying the samples at 105°C at 24-hr intervals until the weight change was less than 5 %. Bulk density is calculated by dividing the weight of the oven-dried sample by the sample volume. Porosity (n) was calculated from the bulk density (ρ_b) data assuming a particle density (ρ_s) of 2.65 kg m^{-3}:

$$n = 1 - \rho_b(\rho_s^{-1}) \qquad (6)$$

Moisture Retention Curves

No single method can cover the entire range in potentials for moisture characteristic curves; therefore, several different methods were used. The main drying (desorption) curve was measured with Tempe pressure cells (0.0 to -0.1 MPa), pressure plate extractors (-0.1 to -1.5 MPa) (Soil Moisture Equipment, Inc.), and a thermocouple psychrometer sample changer (-0.2 to -10 MPa). Hysteresis was ignored. Undisturbed cores that were previously saturated for hydraulic conductivity tests were placed in the Tempe cells to measure matric potential using 0.05 and 0.1 MPa pressures plates. Pressures of 0.02, 0.05, 0.07, and 1.0 MPa were applied using nitrogen gas. Disturbed material was used for characteristic curves below -0.1 MPa because most of the water is adsorbed on the grain surfaces at these matric potentials (Pappendick and Campbell, 1980). Soil samples were saturated on the pressure plates in a water tank by allowing water to rise for approximately 1 day. A paste was made with fine ground soil to ensure a good contact between the soil and the plate. Pressures of 0.15, 0.3, 0.4, 0.5, 0.75, 1.0, and 1.5 MPa were applied, and 0.5 and 1.5 MPa pressure plates were used. Equilibration times ranged from 1 to 7 days depending on the pressure. Gravimetric moisture content of samples was determined after pressure equilibration. Water potentials of samples removed from the pressure chambers were also measured with a thermocouple psychrometer (Decagon Inc.). The retention curves were extended beyond -1.5 MPa (range of the pressure extractors) by air drying the samples and measuring water potential with a laboratory psychrometer and moisture content at various intervals. Characteristic curves of 30 additional soils were measured by air drying the samples and measuring the water potential and gravimetric moisture content. Although the psychrometer measures matric and osmotic potentials whereas the pressure plate measures matric potentials only, chloride concentration data from soils at the site

indicate that the osmotic potential is negligible and that the two potentials should be comparable.

Results

Water Content

Volumetric moisture content monitored with the neutron probe ranges from 1 to 32 % (fig. 14). Porosities of surficial sediments calculated from bulk-density information range from 40 to 56 % (table 2). Moisture content and porosity data of these samples indicate that the surficial material is approximately 10 to 20 % saturated. Porosities of the deeper clays (boreholes 23, 11 - 19 m; borehole 27, 14 - 24 m) (fig. 3) range from 26 to 36 % and average 31 % (14 samples) (Brettmann, 1989). Porosity of deposits at well 22, estimated from litho-density and compensated-neutron logs according to methods outlined in Dewan (1983), average 33 % between depths of 40 and 135 ft (12 to 41 m) in clay beds. Based on these porosity data, the deep clays penetrated by access tubes 18 and 19 are close to saturation. Water contents at shallow depths ranged from 7 to 14 % by volume (fig. 15). Gravimetric moisture contents ranged from 2 to 18 % (figs. 16 and 17). The highest moisture contents were recorded in the shallow subsurface after rainfall events (fig. 16; boreholes 15, 42, and 50). The lowest moisture contents were measured in samples from boreholes 30, 31, and 51 that were drilled in the winter (fig. 17). Volumetric moisture contents cannot be calculated from these data because bulk density information is not available.

Temporal variations in moisture content were evaluated by monitoring with a neutron probe. Monthly monitoring in access tubes 18 and 19 shows that moisture content remains constant with time throughout the section (fig. 14). Similar results were recorded at shallow depths although access tube 61, which is installed in a pond, shows variation in

moisture content from 10 to 14 % down to a depth of approximately 1.3 ft (0.4 m) (fig. 15). It is important to recall that neutron probe data are not valid at depths of less than 1 ft (0.3 m); however, comparison of laboratory gravimetric moisture-content data from borehole 50 (sampled after rainfall) with those from nearby borehole 51 (sampled after a long dry period) shows temporal variations in moisture content down to a depth of 1 ft (0.3 m) (figs. 16 and 17). Wetting fronts were observed after rainfall events down to a 0.5 ft (0.15 m) depth by shallow coring (borehole 41C).

Water Potential

Results from laboratory psychrometric measurements of samples collected in June and July 1988, show that water potential generally increases with depth except in the shallow subsurface after rainfall events (fig. 16). Water potentials ranged from -0.1 to -15.6 MPa. Lowest water potentials were measured in the top meter of soil after rainfall. Highest water potentials were also measured in the shallow zone after long dry periods. Water potential (matric and osmotic) generally approximates the total potential because the gravitational component is negligible (< 1.5 MPa). The osmotic potential is also very small (> -1.6 MPa).

Samples from borehole 21 (fig. 3) were collected after a long dry period and exhibit water potentials that range from -16 MPa near the surface to -1.5 MPa at 30 ft (9 m) depth. The hydraulic gradient is steepest near the surface, approximately -5 MPa m^{-1}, and indicates that there is a potential for upward movement of water. The reversal in the potentials between 16 and 23 ft (5 and 7 m) was not recorded in profiles at boreholes other than 21 and may be an artifact of drying during sample collection. Similar water potentials were recorded in samples from boreholes 41 (-3 to -12 MPa) and 15 (-1 to -12 MPa). Borehole 15 was sampled after a rainfall event; therefore, water potentials near the surface are close to zero and water potentials decrease to -12 MPa within 5 ft (1.5 m). For detailed

examination of the hydraulic gradient near the wetting front, samples were collected at 2-inch (50-mm) intervals in three shallow boreholes (exemplified by borehole 41C (fig. 16)). An increase in water potential from -0.1 to -13.2 MPa within 2 inches (50 mm) of ground surface indicates that the wetting front was very sharp. Water potentials in samples from borehole 50 were higher than those from all the other boreholes between 0.7 and 16 ft (0.2 and 5 m) depth. The lack of samples from borehole 23 between 1 and 6 ft (0.3 and 2 m) makes it difficult to reconstruct the water potential profile in the borehole.

Water potentials of samples collected in the winter from boreholes 30, 31, and 54, ranged from -2 to -8 MPa (fig. 17), which is a smaller range than that measured in samples collected the previous summer (-0.1 to -15.6 MPa). Water potentials in samples from boreholes 30 and 54 showed a decrease in water potential to a depth of approximately 3 ft (1 m) and then a general increase. Water potentials of samples from borehole 31 showed greater variability with depth. Boreholes 56 and 57 were sampled at 2-inch (50-mm) increments at shallow depths. Water potentials from borehole 56 are as low as -12 MPa, similar to those recorded in the summer from borehole 15 (fig. 16). Borehole 57 was drilled in the ephemeral pond (fig. 9) that retained water after rainfall events the previous summer; it shows lower water potentials than those from borehole 56.

The shallow *in situ* psychrometers (< 4.6 ft [1.4 m] depth) that were installed in close contact with the surrounding sediments equilibrated within 1 day, whereas the deeper psychrometers (9 to 47 ft [2.7 - 14.3 m]) installed in the borehole required approximately 20 days to equilibrate (fig. 18). The trend in water potentials during equilibration was from low (-4 to -6 MPa) to high (-2.3 to -3.6 MPa). This trend is as expected because the sediments were dried during installation. The rate of equilibration decreased with time. After equilibration, the water potentials measured by the psychrometer pairs generally aggreed within 0.2 MPa, which indicates that the water potentials are reliable. Water potentials increase with depth, indicating a potential for upward movement of water. Water potentials of the shallow psychrometers (1 ft (0.3 m)) went out of range in 5/12/89 (Julian

day 132). Water potentials in psychrometers at 1.6 and 2.6 ft (0.5 and 0.8 m) show a gradual decrease during the monitoring period. The duration of the monitoring period is insufficient to evaluate seasonal fluctuations in water potential. Diurnal variations in water potential were restricted to the psychrometers at a depth of 1 ft (0.3 m) (fig. 19). The water potential gradient is steepest in the upper 10 ft (3 m) and approaches unity with depth (fig. 20). The gradient also becomes steeper with time in the shallow zone.

Temperature oscillations over time are most pronounced in the shallow zone and decrease with depth (fig. 21). Hourly variations in temperature are primarily restricted to psychrometers at 1 ft (0.3 m) depth (fig. 22). Temperature variations at this depth lag surface temperature variations by approximately 12 hr. The temperature gradients were initially negative upward but reversed direction in early March (fig. 23). Temperature gradients are steepest down to a depth of 16 ft (5 m) and are close to unity below this depth. The gradients have become steeper over the monitoring period, and the depth of penetration of the steep gradients has also increased.

CHEMICAL APPROACH

Chloride concentrations in soil water have been used extensively to evaluate recharge rates in semiarid systems (Peck and others, 1981; Sharma and Hughes, 1985; Johnston, 1987). Chloride is an ideal tracer because it is chemically conservative. Plant uptake is minimal because chloride is a trace nutrient. The theory of chloride transport has been described by Bresler (1973) and Peck and others (1981). Under steady-state conditions, water (q_w) and solute (J_s) fluxes can be described by

$$q_w = - D_w \partial\theta/\partial z + K \qquad (7)$$

and

$$J_s = - D_h \partial C/\partial z + Cq_w \qquad (8)$$

where $D_w = D_w(\theta) = K\,\partial\psi/\partial\theta$ is the soil water diffusivity; θ is the volumetric water content; $K = K(\theta)$ is the hydraulic conductivity; $D_h = D_h(\theta,V)$ is the hydrodynamic dispersion coefficient; C is the concentration; V is the average soil water velocity; and z is the vertical space coordinate. For nonreactive species, conservation of water and solute are

$$\partial\theta/\partial t = -\partial q/\partial z + W \qquad (9)$$

$$\partial(\theta C)/\delta t = \partial J_s/\partial z + S \qquad (10)$$

where W and S are water and solute source terms, respectively. Combining conservation of energy equations (7, 8) with the conservation of mass equations (9, 10) leads to general water-flow and solute-transport equations:

$$\partial\theta/\partial t = \partial(D_w\partial\theta_w/\partial z)\partial z - \partial K/\partial z + W \qquad (11)$$

$$\partial(\theta C)\partial t = \partial(D_h\,\partial C/\partial z)\partial z - q_w\,\partial C/\partial z + S - CW \qquad (12)$$

Under steady-state conditions, $\partial\theta/\partial t$ and $\partial(\theta C)/\partial t$ are zero and q_w can be calculated from equation 8 if J_s, D_h and C are known. Assuming D_h is negligible:

$$q_w = J_s/C \qquad (13)$$

Equation 13 is equivalent to the following equation for chloride:

$$q_w = P \cdot Cl_p / Cl_{sw} \qquad (14)$$

where J_s for chloride is approximated by $P \cdot Cl_p$ (P is the long-term mean annual precipitation rate; Cl_p is the mean chloride concentration of precipitation), and C is approximated by Cl_{sw} (mean chloride concentration in soil water below the root zone) as used by Sharma and Hughes (1985) and Mattick and others (1987). The travel time (t) represented by chloride at depth z can be evaluated by dividing the total chloride mass from the surface to that depth by the chloride flux and can be derived from equation 14:

$$t = \Sigma\, Cl_{sw} \cdot z / P \cdot Cl_p. \qquad (15)$$

Chloride concentrations in soil water are inversely proportional to recharge rates; high chloride concentrations are indicative of low recharge rates. Chloride profiles provide a qualitative estimate of recharge rates because there are many assumptions associated with this method: one-dimensional vertical piston-type flow; precipitation is the only source of

chloride; mean annual precipitation and chloride concentration of precipitation are constant through time; and steady state subsurface flow conditions apply.

This model of chloride movement assumes that chloride concentrations increase through the root zone by evapotranspiration and should remain constant below the root zone. Most chloride profiles described in the literature are bulge shaped and show a reduction in chloride concentration below the root zone. The decrease in chloride concentration has been attributed to (1) dilution from another water source at depth, (2) non-piston flow, or (3) changing climatic conditions through time.

Anthropogenic Radioisotopes

Recharge rates also can be estimated from penetration depths of radioisotopes such as ^{36}Cl, which was enriched in the atmosphere by neutron activation of ^{35}Cl in sea water by weapons tests conducted in the South Pacific between 1952 and 1958 and peaked in 1955 (Bentley and others, 1986). ^{36}Cl has a half life of $3.01 \cdot 10^5$ yr. Natural ^{36}Cl is produced by cosmic-ray spallation of ^{40}Ar and neutron activation of ^{39}Ar (Bentley and others, 1986). The ratio of natural ^{36}Cl to stable chloride (^{35}Cl or Cl) in the study area is approximately $5.0 \cdot 10^{-13}$ (fig. 24). Temporal variations in ^{36}Cl fallout can be predicted with an atmospheric box model (fig. 25). Latitudinal variation in ^{36}Cl can be evaluated using ^{185}W, which indicates that ^{36}Cl fallout in southwestern U.S., including the study area, was approximately $3.4 \cdot 10^{-12}$ atoms/m^2 (Phillips and others, 1989).

Field Methods

Approximately 200 samples were collected for moisture content and chloride analysis in 9 boreholes drilled during July and August 1988, and in January and February 1989. Collection of undisturbed samples for volumetric moisture content analyses was nearly

impossible because the material was not cohesive. The sampling interval varied from approximately 1 to 3 ft (0.3 to 1 m). Borehole 18 was drilled with a wireline drill rig using air as a circulation fluid for installation of a neutron access tube, and samples were collected with a split spoon to 70 ft (21 m). The remaining boreholes were rotary drilled with hollow-stem augers, and samples were collected in shelby tubes. No drilling fluids were used. These boreholes were drilled until auger refusal, which generally occurred at the top of the clay. Boreholes 23 and 27 were further deepened with a wireline drill rig for geotechnical purposes. Approximately 80 g of sample was collected for moisture and chloride analysis. Samples were placed in PVC sample cups, sealed with parafilm and tape to prevent moisture loss, and weighed in the field.

In addition to samples for moisture content and chloride analyses, 26 samples were collected for ^{36}Cl analysis in January 1989. The sampling interval was predetermined from chloride profiles, which suggested that soil water to a depth of 1.6 ft (0.5 m) accumulated during the last 30 yr. Collection of discrete samples is important to adequately define the peak; therefore, five samples were collected above the predicted peak depth. Samples were collected at 0.3 ft (0.1 m) intervals to 3 ft (1 m) from a shallow pit dug with a trowel and stored in plastic garbage bags. The amount of sample required was calculated from chloride-concentration data. Samples from depths greater than 3 ft (1 m) were collected with shelby tubes in a hollow-stem auger and placed in mason jars. Subsamples for moisture content and chloride analysis were sealed in plastic cups with parafilm and tape.

Laboratory Methods

Gravimetric moisture content was determined by drying approximately 80 g of soil at 105°C until the weight loss was less than 5 % (approximately 48 hr). Double-deionized water was added to the dried sample in a 1:1 or 2:1 ratio. Samples were placed on a reciprocal shaker table for 8 hr and then centrifuged for 10 min at 5,000 revolutions per

minute. The supernatant was filtered through 0.45 μm filters and then analyzed for chloride by ion chromatography or by potentiometric titration. To test whether oven drying had any effect on chloride concentration, four samples were split and two were oven dried. Comparison of the chloride concentrations of the splits showed that oven drying had no effect on chloride concentrations; therefore, the other two samples were oven dried.

Laboratory preparation of ^{36}Cl samples generally followed procedures outlined in Mattick and others (1987). The amount of soil varied from 10 kg at the surface to 1 kg at depth. Double-deionized water was added and the mixture stirred with an electric stirrer for approximately 12 hr. $AgNO_3$ was added to the chloride solution to precipitate AgCl. ^{36}S is a competing isobar of ^{36}Cl. The AgCl was purified of ^{36}S isobar by adding $Ba(NO_3)_2$. Isotopic ratios of samples from the top meter were diluted in a 1:1 ratio with dead carrier in one split of the samples because $^{36}Cl/Cl$ ratios of less than 1,000 are preferred for analysis with the Tandem Accelerator Mass Spectrometer (TAMS), and measured peak ratios of bomb $^{36}Cl/Cl$ are up to 20,000 in some areas (Phillips and others, 1989). The dead carrier obtained from the University of Rochester, consisted of Weeks Island halite from Louisiana. The dead carrier was put through the same purification procedure as that of the soil samples to evaluate chemical contamination during sample preparation. The AgCl samples were wrapped in aluminum foil to prevent reduction of Ag^+ to Ag.

The $^{36}Cl/Cl$ ratios were measured by TAMS at the University of Rochester (Elmore and others, 1979). The AgCl samples were loaded in 0.06 inch- (1.6-mm) diameter cups. Because the measurements take approximately 1 to 2 hr per sample, the 10 uppermost samples that had been diluted with dead carrier were scanned to determine the approximate position of the bomb peak, to evaluate ^{36}S interference, and to determine if the ratios were greater than 10,000. All ratios were less than 5,000. In 5 of the 10 samples ^{36}S contamination was a problem and may have resulted from the use of latex gloves during sample loading. These samples were reloaded from different vials. Each run consisted of four samples, two standards, and a University of Rochester blank. The standards used had

a ratio of 1,600. Twelve samples and a blank were run. Results from the Weeks Island halite blank indicated that no chemical contamination had occurred during sample processing.

Results

The chloride profiles display a variety of shapes; however, all may be generally characterized as bulge shaped (fig. 26). The bulge profiles generally consist of low concentrations near the surface (generally at depths of less than 1 ft [0.3 m]). Concentrations increase to a maximum at depths from 4.3 and 15 ft (1.3 and 4.6 m) and then decrease to a constant low concentration at depths of greater than 20 ft (6 m). Maximum chloride concentrations range from 1,900 to 6,300 g/m^3. Peak chloride concentrations in samples from boreholes 27 (5,100 g/m^3) and 30 (6,300 g/m^3) are much higher than those recorded in samples from all other boreholes (1,900 to 3,300 g/m^3). Because chloride concentrations are inversely proportional to recharge rates, these high chloride concentrations are indicative of very low recharge rates.

The $^{36}Cl/Cl$ ratio is $4.63 \cdot 10^{-15}$ below 4 ft (1.25 m), and this value is similar to the natural fallout ($500 \cdot 10^{-15}$) calculated by Bentley (1986) (fig. 27). The total inventory of bomb Cl is $2.6 \cdot 10^{12}$ atoms/m^2, which is 75 % of that predicted ($3.4 \cdot 10^{12}$ atoms/m^2) (Phillips and others, 1989). The maximum $^{36}Cl/Cl$ ratio was measured at 1.6 ft (0.5 m). The net infiltration to a depth of 1.6 ft (0.5 m) is approximately 0.08 inch (2 mm)/a, which represents approximately 1 % of the mean annual precipitation rate in the region. The actual recharge rate probably is much less than 0.08 inch (2 mm)/a because much of the water below 1.6 ft (0.5 m) will be removed by plant roots.

ACKNOWLEDGMENTS

This research was funded by the Texas Low-Level Waste Disposal Authority. The conclusions presented in this report are not necessarily endorsed or approved by the Authority.

The manuscript was reviewed by A. R. Dutton and T. F. Hentz. Illustrations were drafted by Joel L. Lardon and Kerza Prewitt under the supervision of R. L. Dillon. The report was word processed by the senior author and Melissa Snell and edited by Amanda R. Masterson.

REFERENCES

Akhter, Saleem, 1989, Surface-water hydrology of proposed Texas low-level radioactive waste isolation site: The University of Texas at Austin, Bureau of Economic Geology, report prepared for Texas Low-Level Radioactive Waste Disposal Authority, 44 p.

Bentley, H. W., Phillips, F. M., and Davis, S. N., 1986, ^{36}Cl in the terrestrial environment, *in* Fritz, P., and Fontes, J.-C., (eds.), Handbook of environmental isotope geochemistry, v. 2b, New York, Elsevier Science, p. 422-475.

Bresler, E., 1973, Anion exclusion and coupling effects in nonsteady transport through unsaturated soils: I. Theory: Soil Science Society of America Proceedings, v. 37, p. 663-669.

Brettmann, T. T., 1989, Geotechnical engineering properties of soils at a proposed low-level radioactive waste disposal site in Hudspeth County, Texas: The University of Texas at Austin, Master's thesis, 134 p.

Briscoe, R. D., 1984, Thermocouple psychrometers for water potential measurements, *in* Proceedings of the NATO Advanced Study Institute on 'Advanced Agricultural Instrumentation,' Ciocco, Italy, p. 1-14.

Brown, R. W., and Bartos, D. L., 1982, A calibration model for screen-caged Peltier thermocouple psychrometers: U.S. Department of Agriculture, Forest Research Paper INT 293, p. 1-24.

Brown, R. W., and van Haveren, B. P. (eds.), 1972, Psychrometry in water relations: Logan, Utah State University, Utah Agricultural Experiment Station, 342 p.

Campbell, G. S., 1985, Soil physics with basic: transport models for soil-plant systems: New York, Elsevier, Developments in Science 14, 150 p.

Dewan, J. T., 1983, Essentials of modern open-hole log interpretation: Tulsa, Oklahoma, Penwell Publishing Co., 361 p.

Elmore, D., Fulton, B. R., Clover, M. R., Marsden, J. R., Gove, H. E., Naylor, H., Purser, K. H., Kilius, L. R., Beukens, R. P., and Litherland, A. E., 1979, Analysis of ^{36}Cl in environmental water samples using an electrostatic accelerator: Nature, v. 227, p. 22-25.

Gustavson, T. C., 1989, Sedimentary facies, depositional environments, and paleosols of the Upper Tertiary Fort Hancock Formation and the Tertiary-Quaternary Camp Rice Formation, Hueco Bolson, West Texas: The University of Texas at Austin, Bureau of Economic Geology, report prepared for Texas Low-Level Radioactive Waste Disposal Authority, 93 p.

Johnston, C. D., 1987, Distribution of environmental chloride in relation to subsurface hydrology: Journal of Hydrology, v. 94, p. 67-88.

Lang, A. R. G., 1967, Osmotic coefficients and water potentials of sodium chloride solutions from 0 to 40 C: Australian Journal of Chemistry, v. 20, p. 2017-2023.

Larkin, T. J., and Bomar, G. W., 1983, Climatic atlas of Texas: Texas Department of Water Resources Publication LP-192, 151 p.

Marthaler, H. P., Vogelsanger, W., Richard, F., and Wierenga, P., 1983, A pressure transducer for field tensiometers. Soil Science Society of America Journal, v. 47, p. 624-627.

Mattick, J. L., Duval, T. A., and Phillips, F. M., 1987, Quantification of groundwater recharge rates in New Mexico using bomb 36Cl, bomb 3H and chloride as soil-water tracers: New Mexico Water Resources Research Institute, Research Report 220, 184 p.

Mullican, W. F. III, Kreitler, C. W., Senger, R. K., and Fisher, R. S., 1989, Truly deep saturated zone investigations at the proposed low-level radioactive waste disposal site for Texas, *in* Proceedings of the Third National Outdoor Action Conference on Aquifer Restoration, Ground Water Monitoring and Geophysical Methods: National Water Well Association, p. 447-461.

Office of the Federal Register, 1987, Code of Federal Regulations, 10, p. 672-678.

Pappendick, R. I., and Campbell, G. S., 1980, Theory and measurement of water potential, *in* Water Potential Relations in Soil Microbiology: Madison, Wisconsin, Soil Science Society of America, p. 1-22.

Peck, A. J., Johnston, C. D., and Williamson, D. R., 1981, Analyses of solute distributions in deeply weathered soils: Agricultural Water Management, v. 4, p. 83-102.

Phillips, F. M., Mattick, J. L., and Duval, T. A., 1989, Chlorine-36 and tritium from nuclear weapons fallout as tracers for long-term liquid movement in desert soils: Water Resources Research, v. 24, no. 11, p. 1877-1891.

Rawlins, S. L., and Campbell, G. S., 1986, Water potential: thermocouple psychrometry, *in* Black, C. A., Evans, D. D., White, J. L., Ensminger, L. E., and Clark, F. E., (eds.), Methods of soil analysis, part 1, physical and mineralogical methods: Agronomy Monograph No. 9, p. 597-617.

Robinson, R. A., and Stokes, R. H., 1959, Electrolyte solutions: London, Butterworths, 571 p.

Sharma, M. L., and Hughes, M. W., 1985, Groundwater recharge estimation using chloride, deuterium and oxygen-18 profiles in the deep coastal sands of western Australia: Journal of Hydrology, v. 81, p. 93-109.

Siefken, D., Pangburn, G., Pennifill, R., and Starmer, R. J., 1982, Site suitability, selection and characterization: Washington, D.C., U.S. Nuclear Regulatory Commission, NUREG-0902, 26 p.

Spanner, D. C., 1951, The Peltier effect and its use in the measurement of suction pressure: Journal of Experimental Botany, v. 11, p. 145-168.

U. S. Nuclear Regulatory Commission, Office of Nuclear Material Safety and Safeguards, 1987, Standard review plan for the review of a license application for a low-level radioactive waste disposal facility: safety analysis report, NUREG-1200.

Van Bavel, C. H. M., Underwood, N., and Swanson, R. W., 1956, Soil moisture measurement by neutron moderation: Soil Science, v. 82, p. 29-41.

Watson, K. K., 1966, An instantaneous profile method for determining the hydraulic conductivity of unsaturated porous materials: Water Resources Research, v. 2, p. 709-715.

Table 1. Osmotic potentials of NaCl solutions (Lang, 1967) and temperatures used in calibration of *in situ* psychrometers.

Temperature (°C)	15.00	20.00	25.00
NaCl (molality)		Water Potential (MPa)	
0.2	0.88	0.90	0.92
0.5	2.20	2.24	2.28
0.7	3.09	3.15	3.21
1	4.46	4.55	4.64
1.5	6.84	6.99	7.13

Table 2. Summary of wells drilled, type of samples collected, and monitoring equipment installed.

Borehole No.	Date Drilled	Total Depth (ft)	No. Samples	Type of Analysis	Monitoring Equipment
15	7/26/88	36	22	water potential	soil solution
	7/27/88		38	moisture content	sampler
			38	chloride	
18	6/27/88	70	22	moisture content	neutron probe
	6/30/88			chloride	access tube
19	6/30/88	135			neutron probe access tube
20	3/17/89	48			in situ psychrometers
21	6/27/88	67	12	water potential	
	7/6/88		24	moisture content	
			24	chloride	
23	7/19/88	80	14	water potential	
	7/25/88		13	moisture content	
			13	chloride	
27	7/21/88	80	22	moisture content	
	8/5/88		22	chloride	
30	1/25/89	48	22	water potential	
	1/28/89		22	moisture content	
			22	chloride	
31	1/29/89	31	20	water potential	
	1/31/89		17	moisture content	
			17	chloride	
41	7/6/88	32	6	water potential	
	7/8/88				
41C	7/11/88	1	6	water potential	
41D	7/11/88	0.8	5	water potential	
42	7/12/88	6	10	water potential	
50	7/14/88	43	25	water potential	
	7/15/88		23	moisture content	
			23	chloride	
51	2/1/89	14	22	moisture content	
54	2/2/89	15	18	water potential	
56	2/2/89	1.6	10	water potential	
57	2/2/89	1		water potential	
61	4/5/89	6			neutron probe access tube
62	4/5/89	6			neutron probe access tube

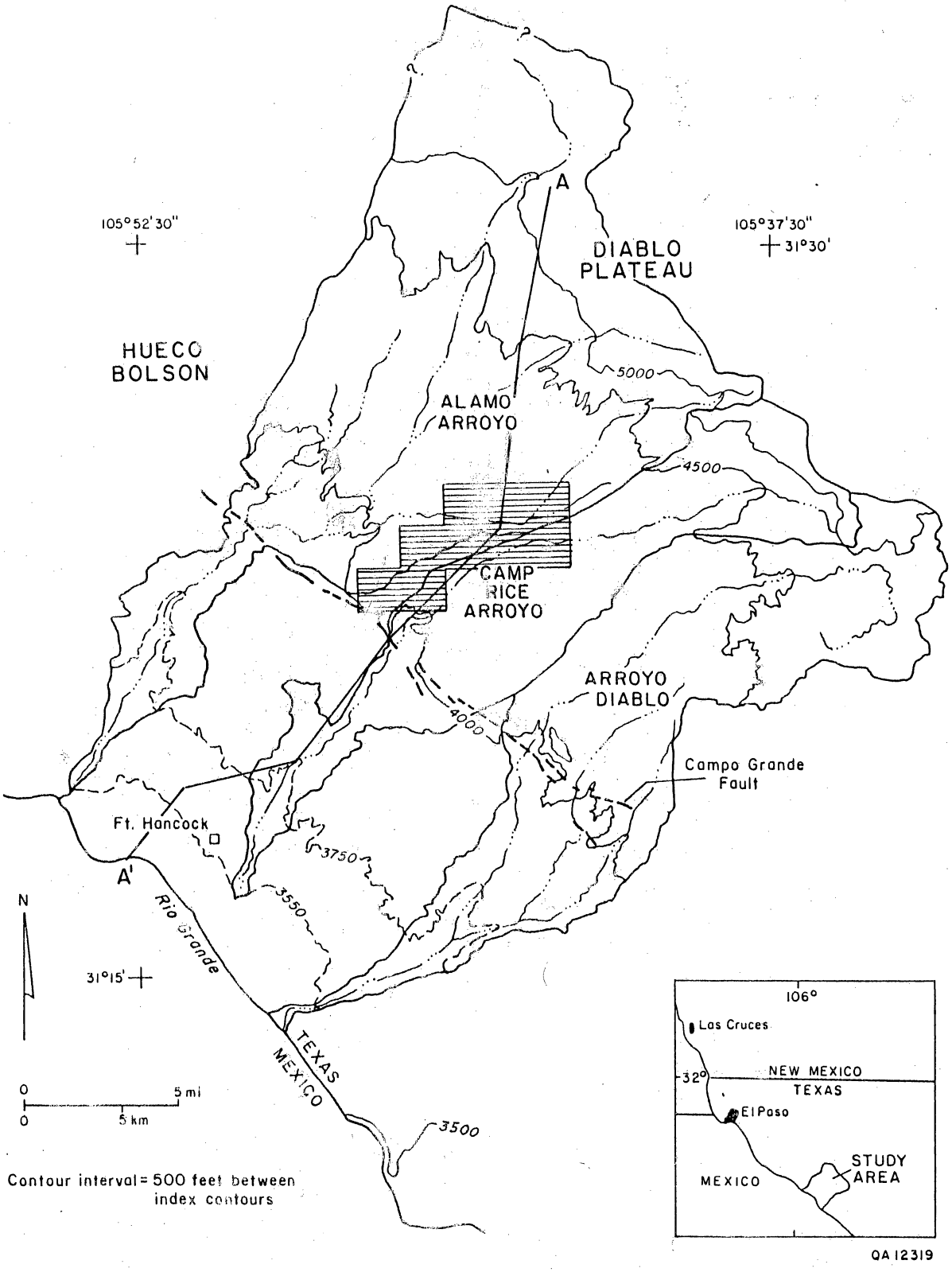

Figure 1. Location of study area.

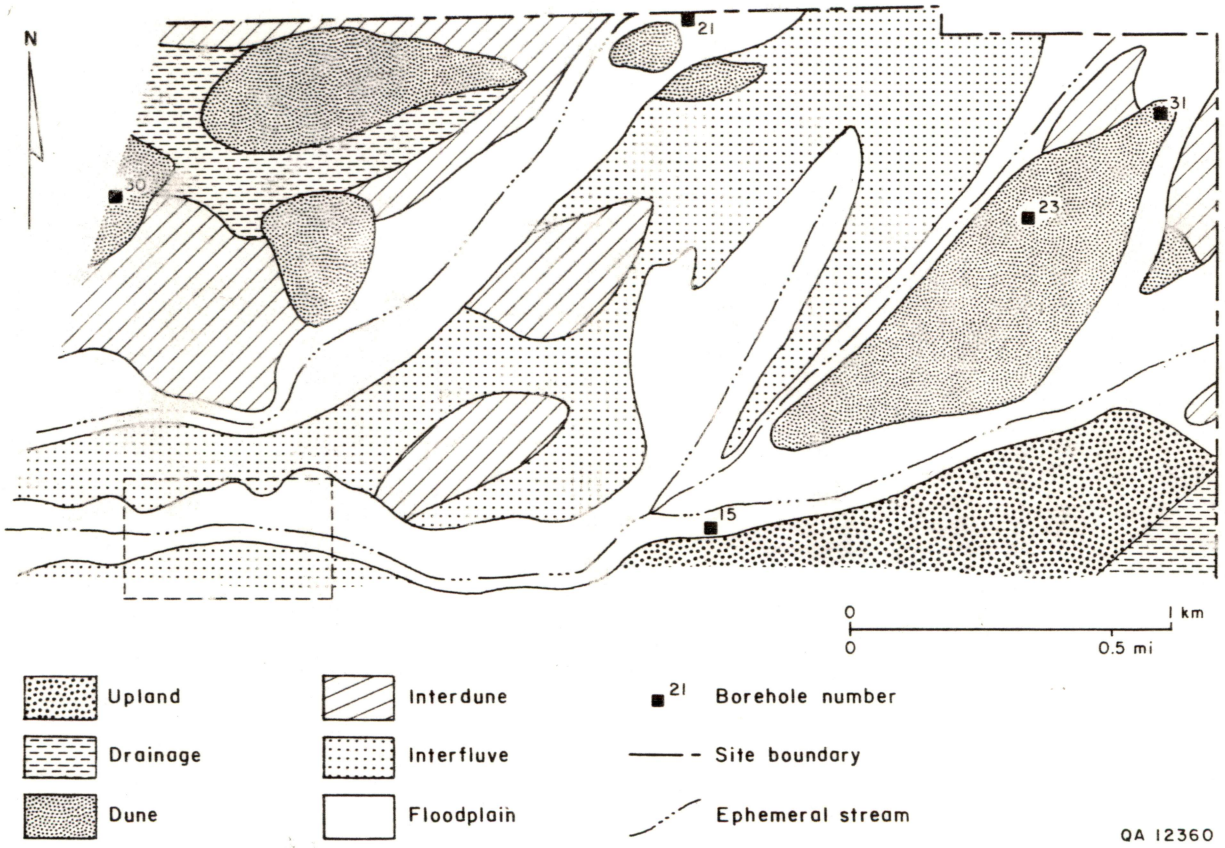

Figure 3. Location of sampled boreholes and unsaturated zone monitoring equipment in the study area. Box in southwestern corner of study map is shown on inset map 8.

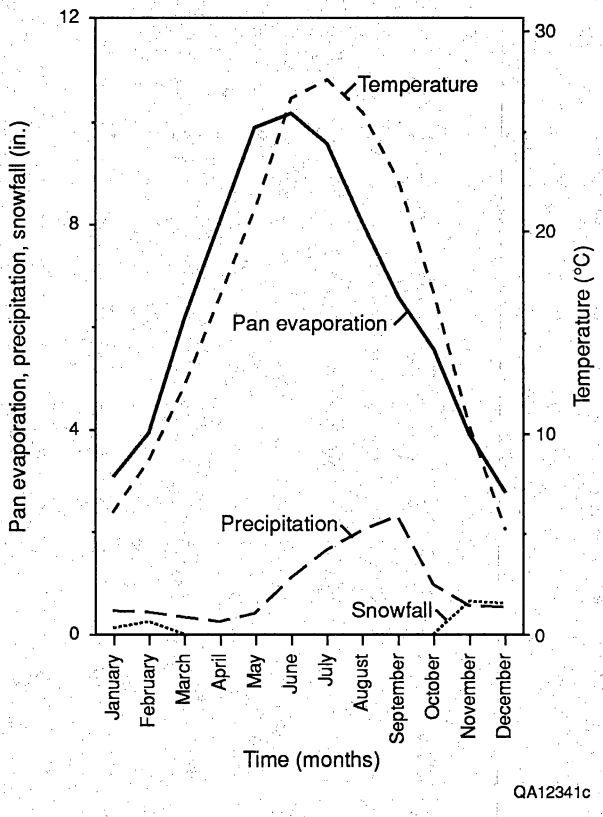

Figure 4. Mean monthly snowfall, precipitation, and temperature recorded in Fort Hancock and mean monthly pan evaporation recorded in El Paso. Monthly means were calculated from meteorological data collected between 1966 and 1987.

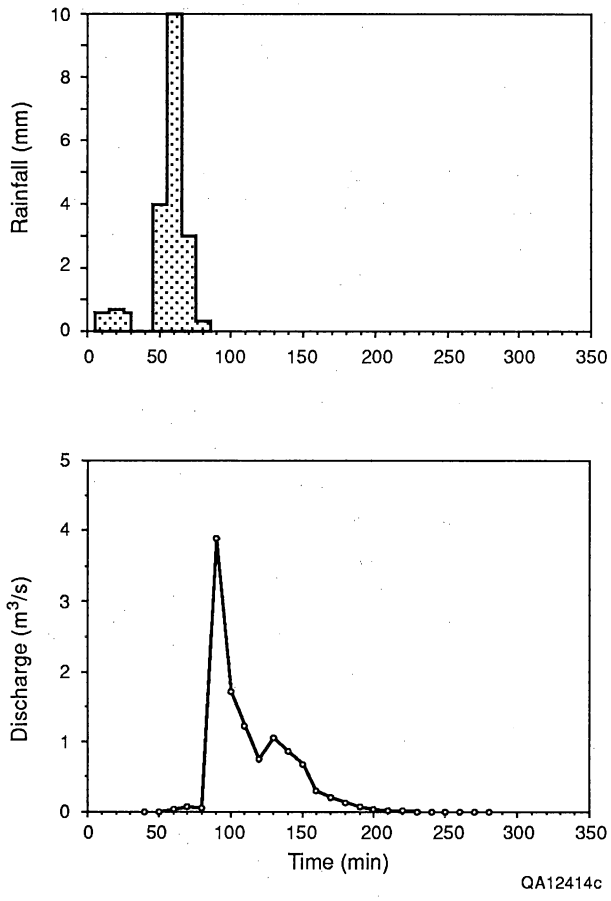

Figure 5. Stream flow hydrograph after an intense rainfall in July 1988 (Akhter, 1989).

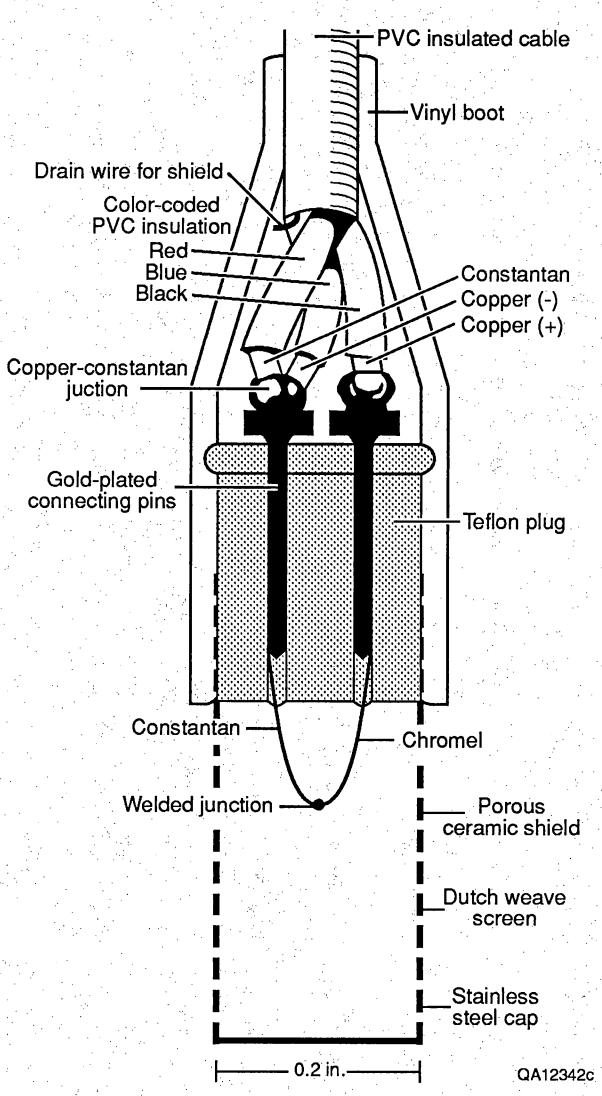

Figure 6. Screen caged, single junction, Peltier thermocouple psychrometer modified from Briscoe (1984).

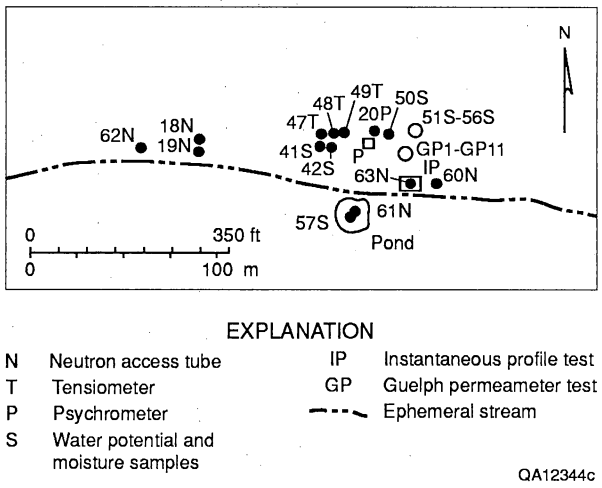

Figure 8. Inset map 8. Detail of unsaturated zone studies including sampled boreholes, monitoring equipment, and hydraulic conductivity tests in ephemeral stream.

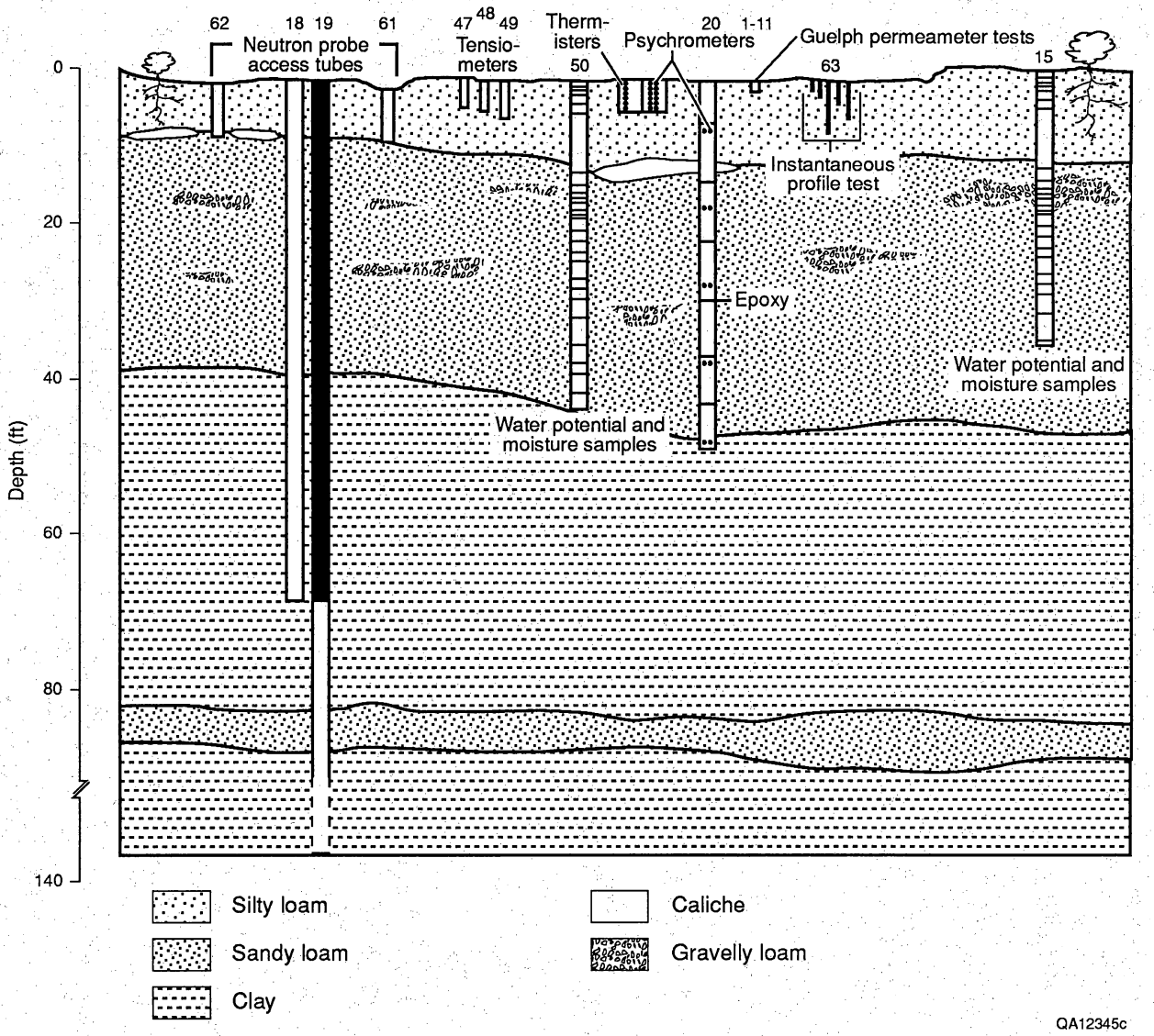

Figure 9. Schematic cross section detailing vertical distribution of monitoring equipment and sampled boreholes. This cross section generally represents studies depicted in figure 8.

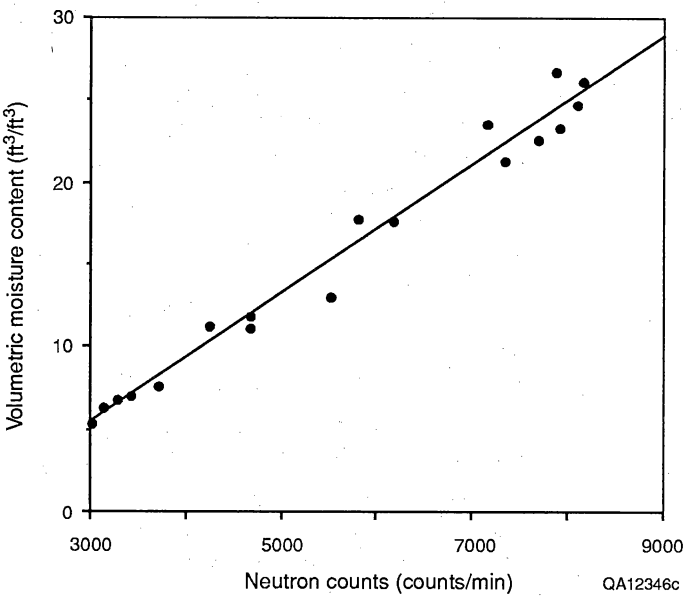

Figure 10. Calibration curve that relates water content to neutron count.

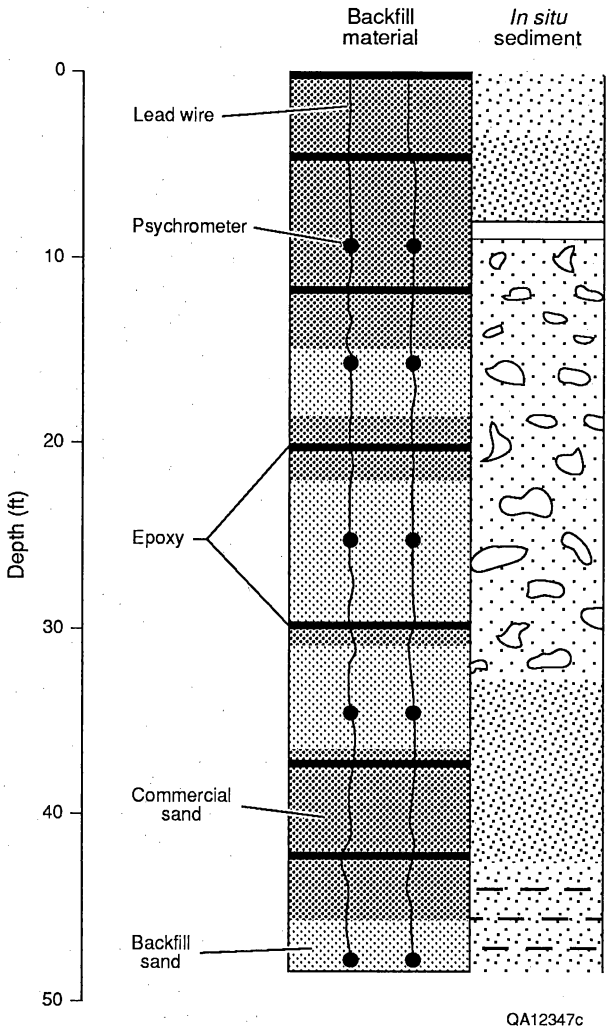

Figure 11. Distribution of psychrometers in borehole 20. Also shown are *in situ* sediments and infill material.

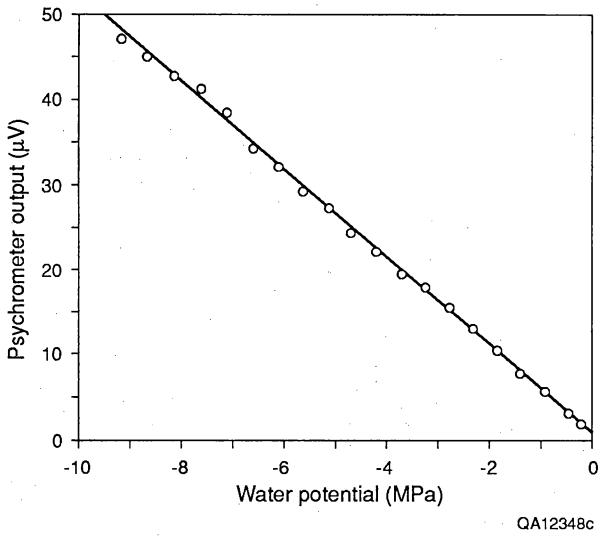

Figure 12. Calibration curve that relates SC-10 thermocouple psychrometer output (µV) to water potential (MPa). Two sets of NaCl standards are represented. Temperature was corrected to 25° C.

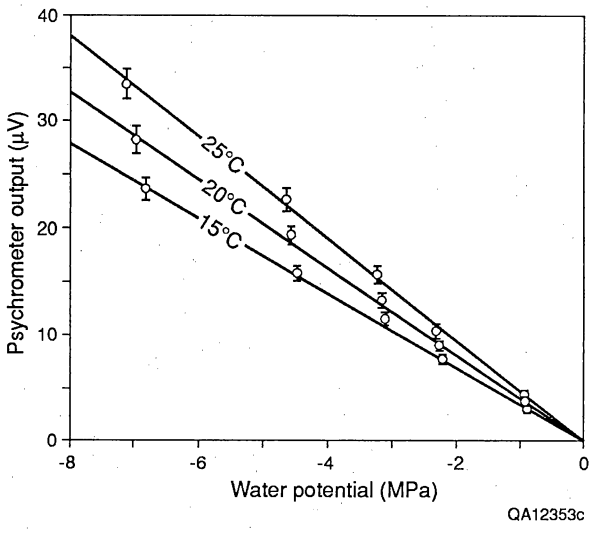

Figure 13. Calibration curve that relates thermocouple psychrometer output (μV) to water potential (MPa). The curve was determined by least-squares linear regression using the mean output from 24 psychrometers. Bar shows ±1 standard deviation of output.

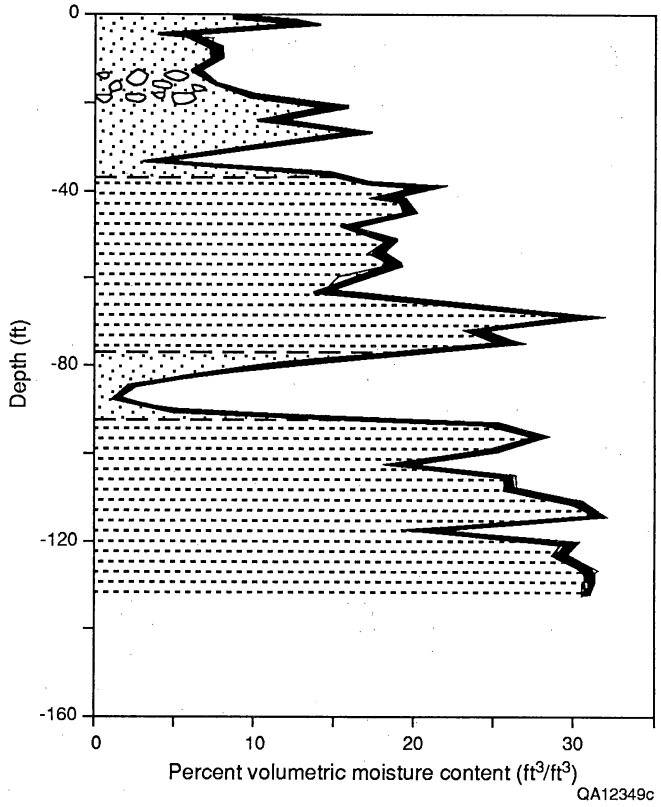

Figure 14. Variation in moisture content with depth and time monitored in access tubes 18 and 19. Moisture content was monitored approximately monthly between July 1988, and July 1989, and 12 are represented. The relationship between moisture content and lithology is also shown. For location of access tubes, see figure 8.

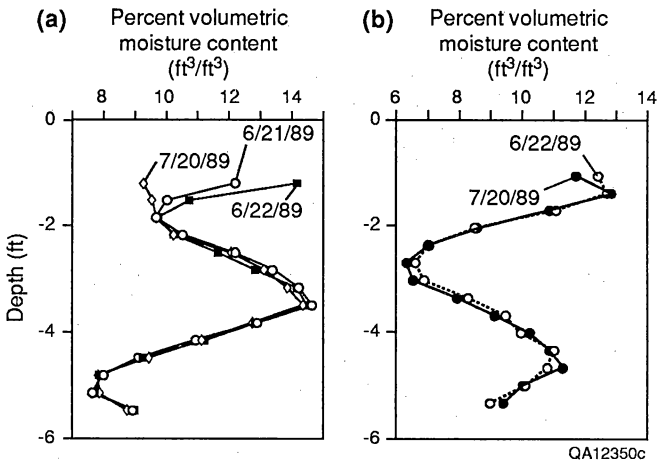

Figure 15. Variation in moisture content with depth and time monitored in access tubes 61 and 62. For location of access tubes, see figure 8.

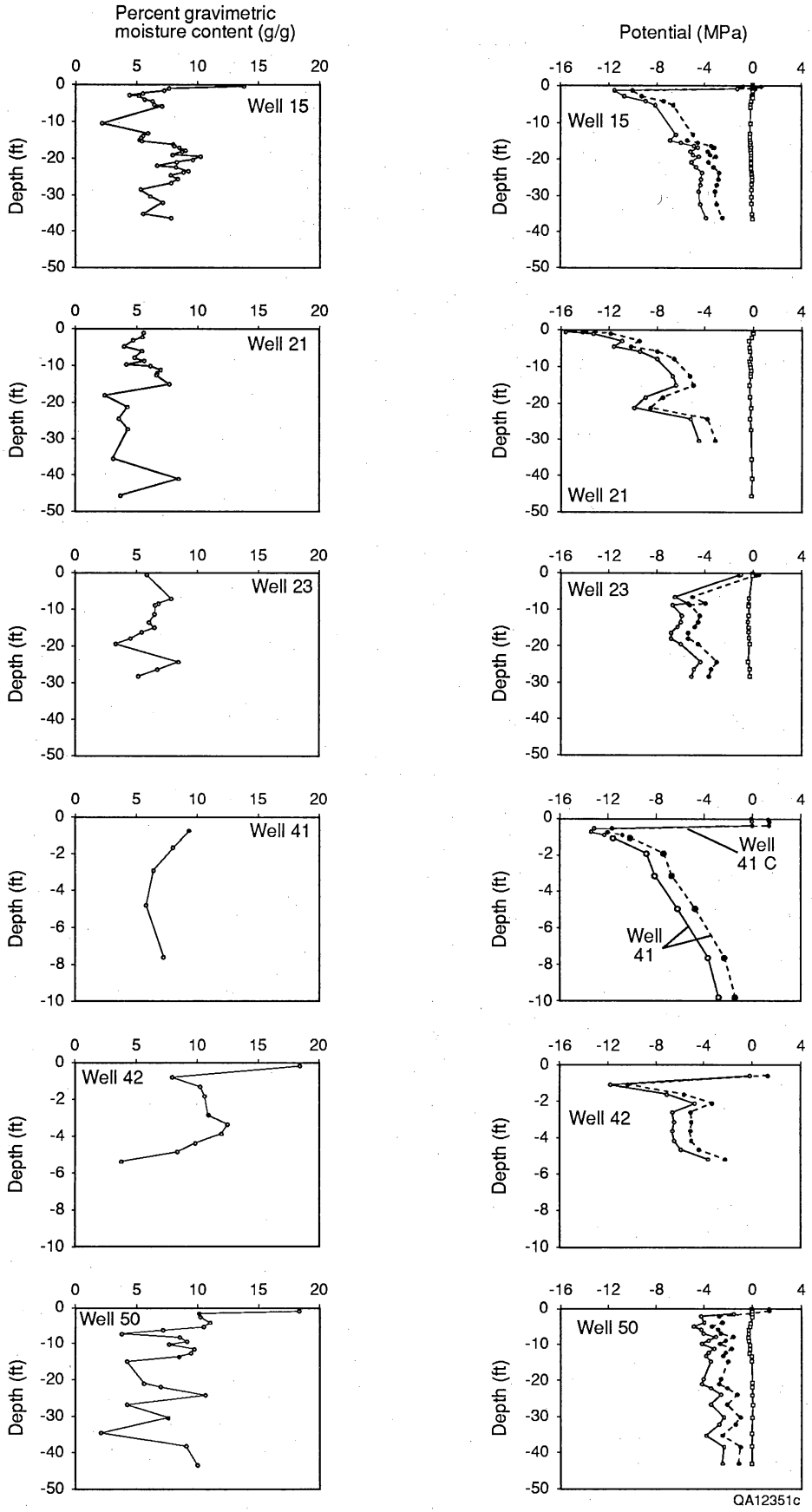

Figure 16. Profiles of gravimetric moisture content and water potential for samples from boreholes 15, 21, 23, 41, 42, and 50 and water potential in 41C. All samples were collected in July and August 1988. For location of boreholes, see figures 3 and 8.

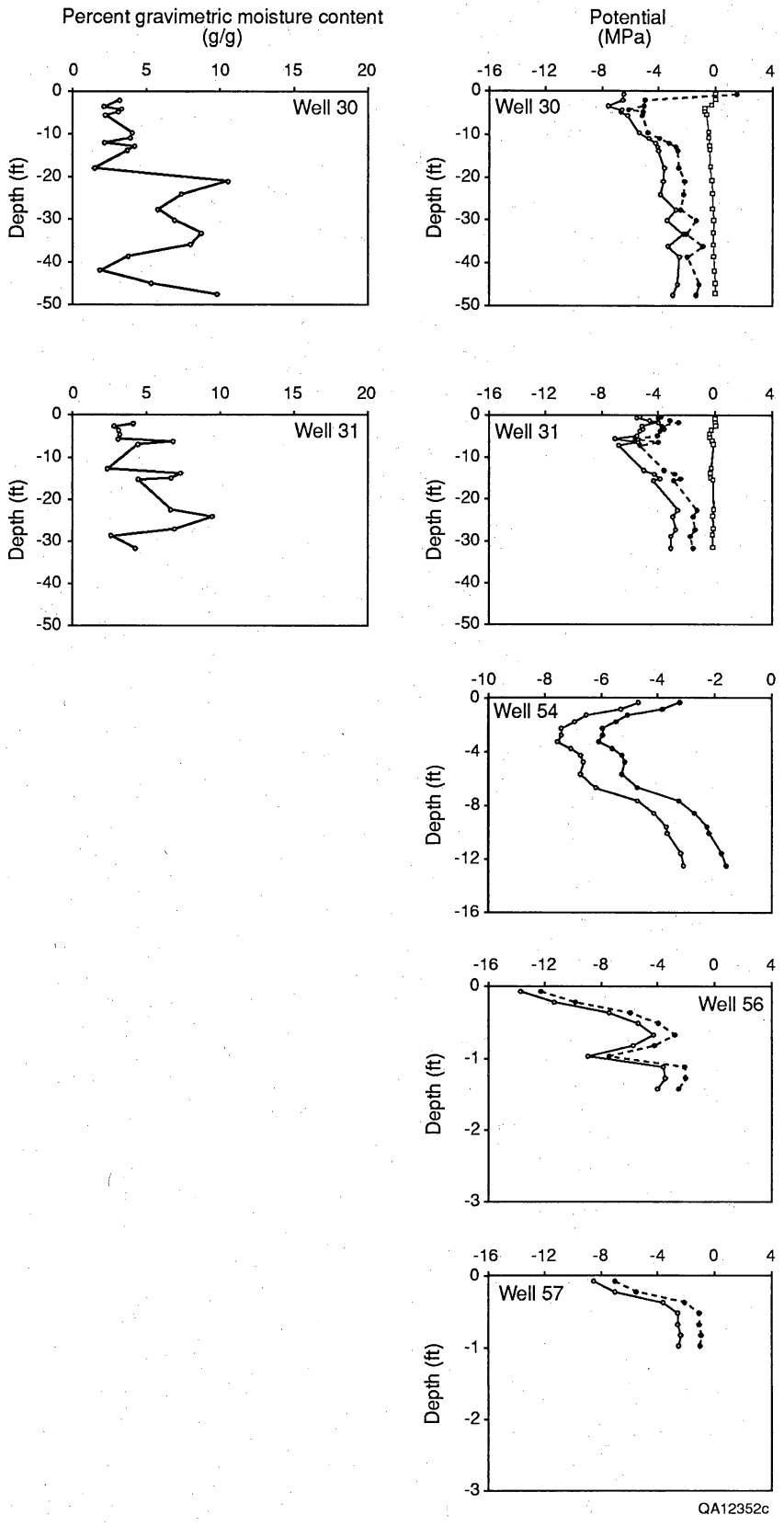

Figure 17. Profiles of gravimetric moisture content and water potential for samples from boreholes 30, 31, and water potential for samples from boreholes 54, 56, and 57. All samples were collected in January and February 1989. For locations of boreholes, see figures 3 and 8.

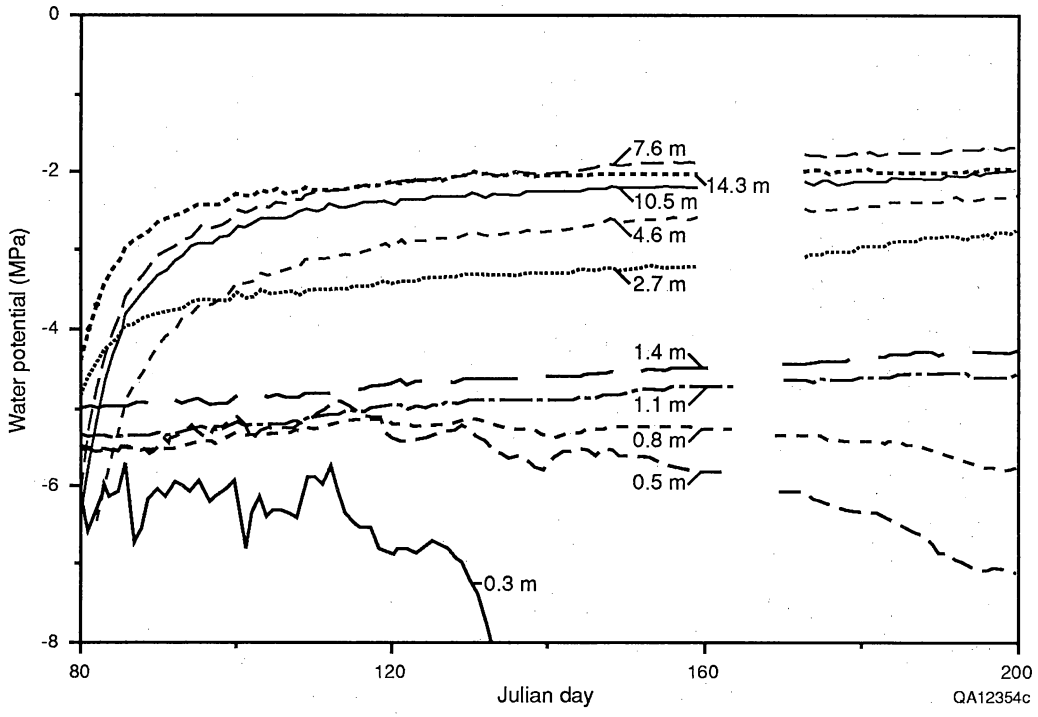

Figure 18. Temporal variations in water potential measured daily at 0900 hours in borehole 20. For location of borehole, see figure 8.

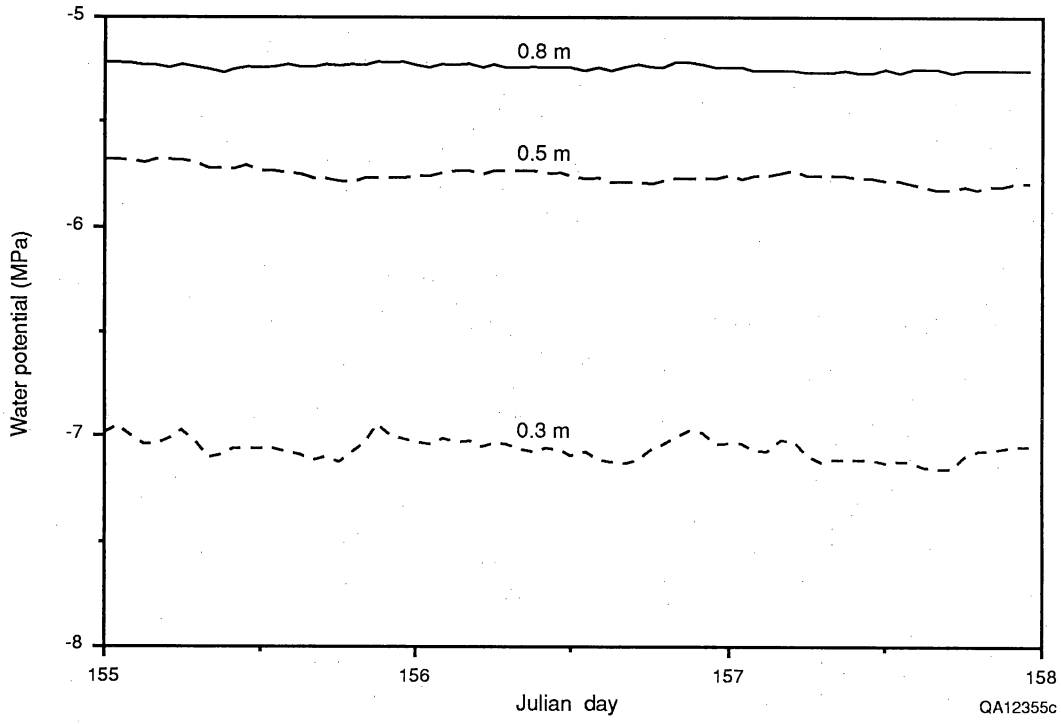

Figure 19. Hourly variations in water potential measured during June 4 to June 6, 1989, in borehole 20.

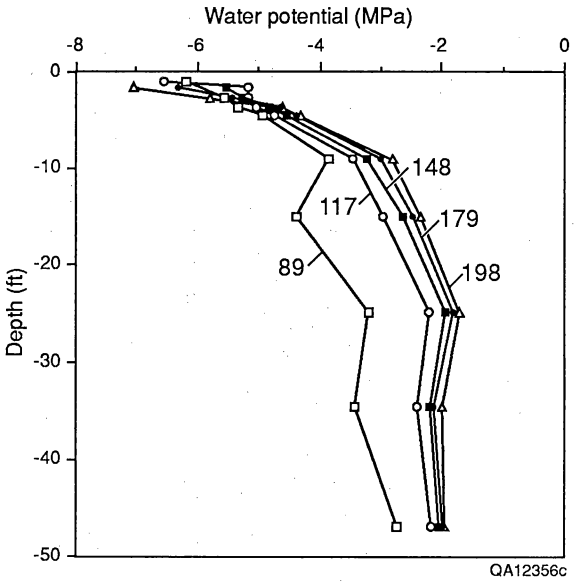

Figure 20. Vertical distribution of water potentials measured between March 30 and July 17, 1989, in borehole 20. Profiles are labeled in Julian days.

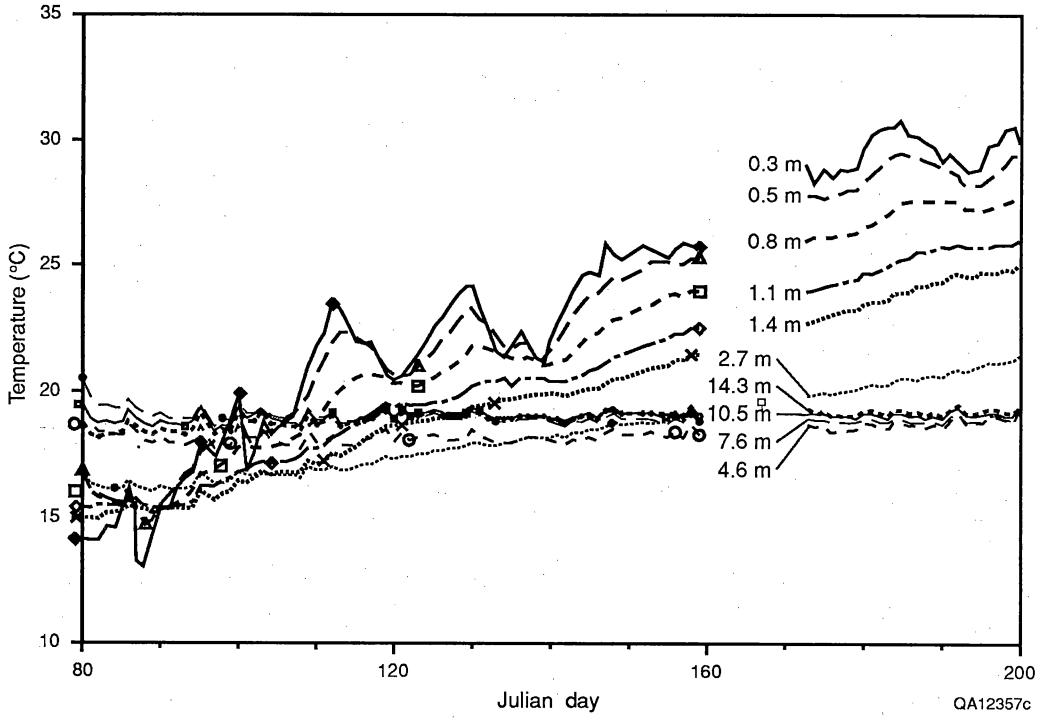

Figure 21. Temporal variations in temperature measured daily at 0900 hours in borehole 20.

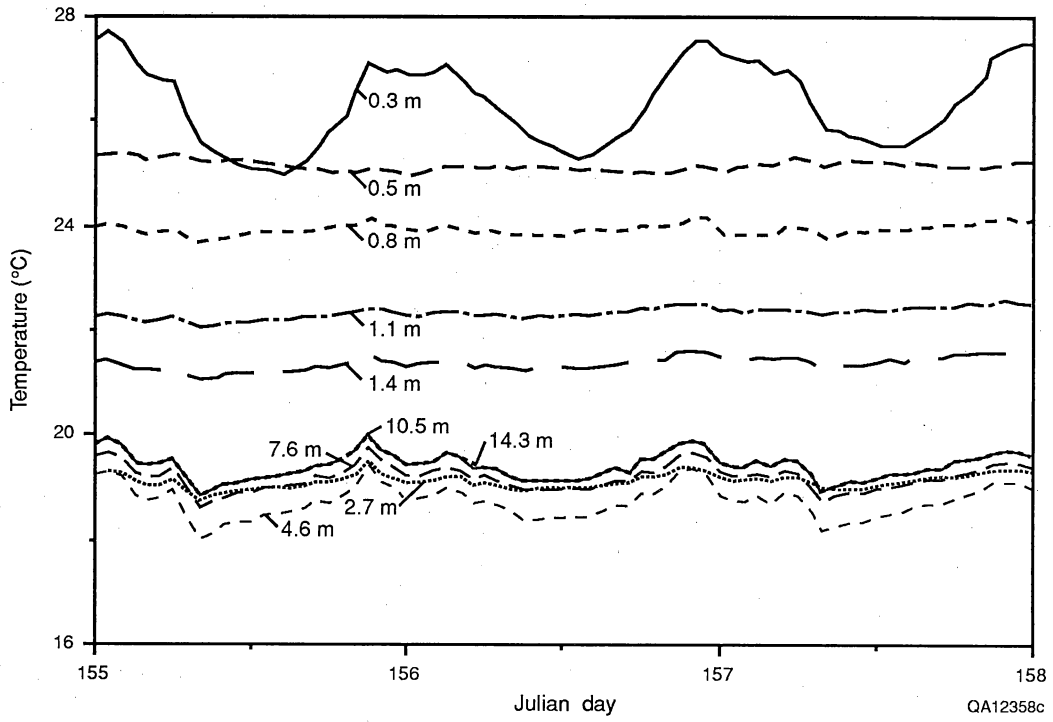

Figure 22. Hourly variations in temperature measured during June 4 to June 6, 1989, in borehole 20.

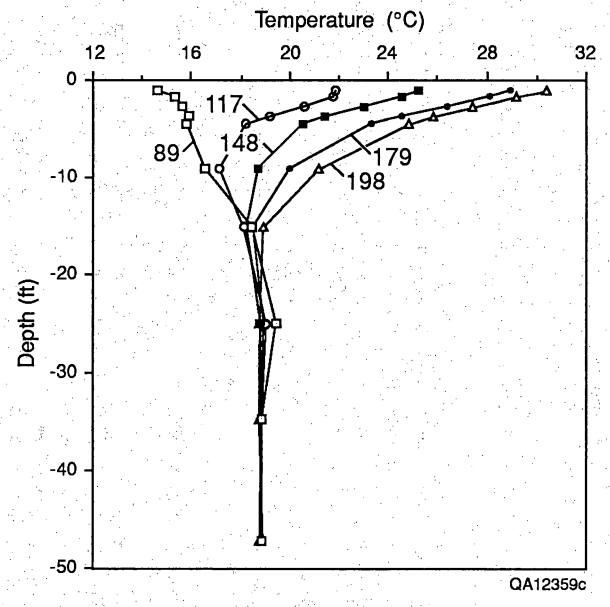

Figure 23. Vertical distribution of temperature measured between March 30 and July 17, 1989, in borehole 20. Profiles labeled in Julian days.

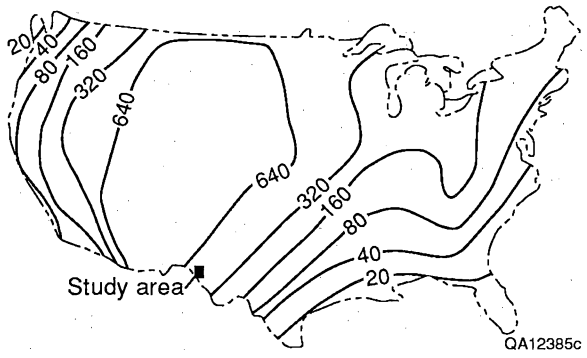

Figure 24. Pre-bomb $^{36}Cl/Cl$ fallout ratios calculated with an atmospheric box model (Bentley and others, 1986).

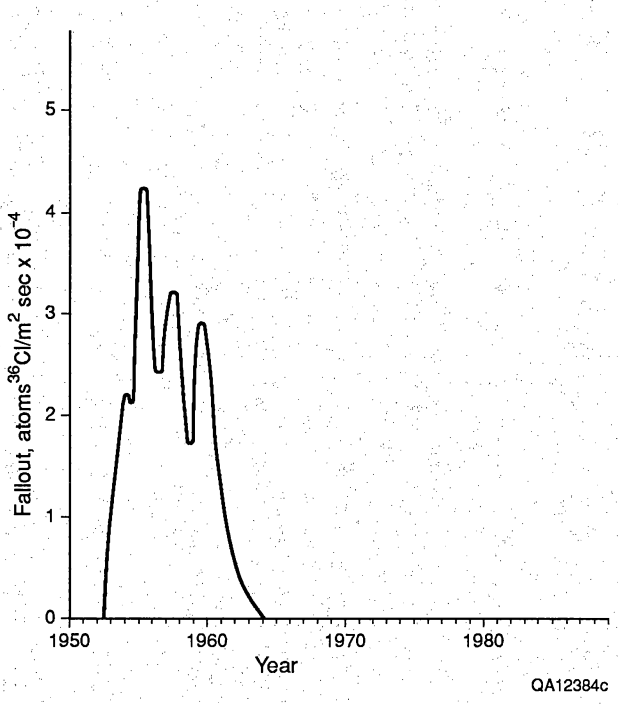

Figure 25. Temporal variations in bomb fallout between 30°N and 50°N latitude (Bentley and others, 1986).

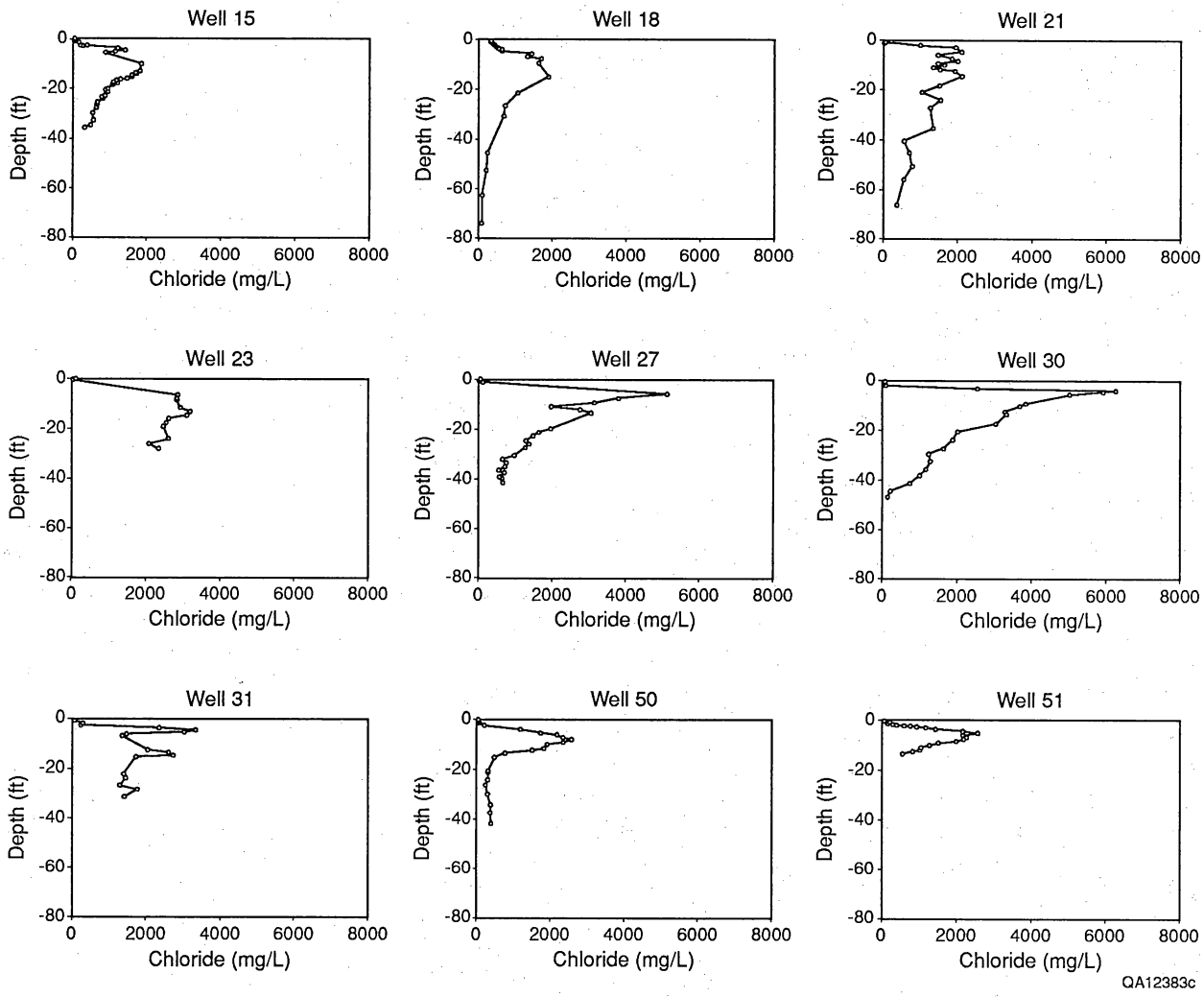

Figure 26. Chloride concentrations of samples from boreholes 15, 18, 21, 23, 27, 30, 31, 50, and 51. For locations of boreholes, see figures 3 and 8.

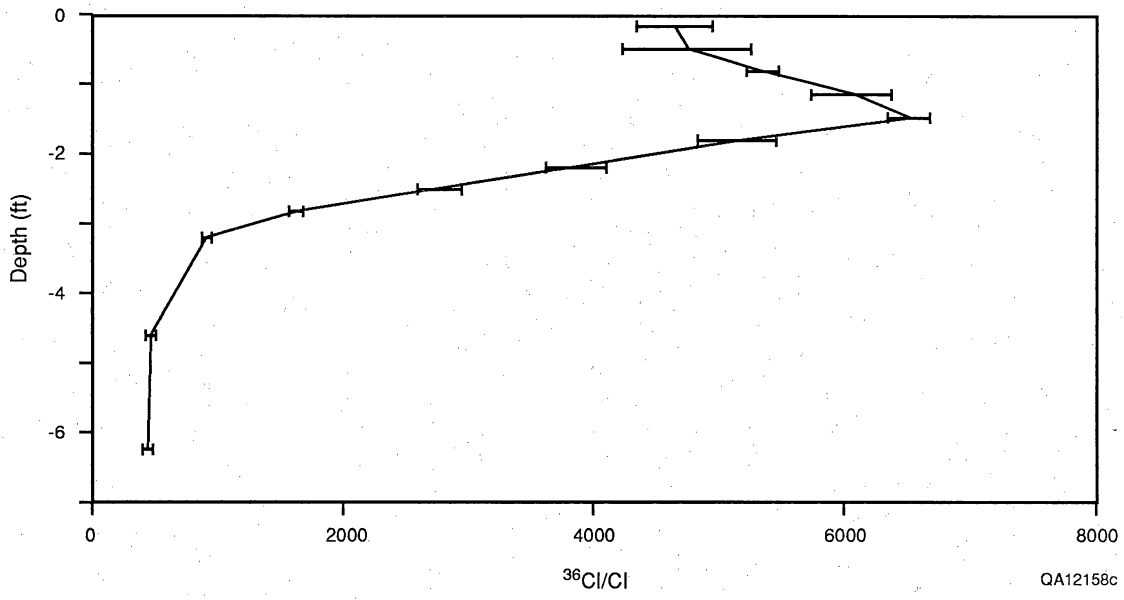

Figure 27. Vertical profile of $^{36}Cl/Cl$ ratios.